

# The Use of Cluster Analysis to Assess the Wear Resistance of Cermet Coatings Sprayed by High Velocity Oxy-Fuel on Magnesium Alloy Substrate

Ewa Jonda<sup>1\*</sup>, Dariusz Fydrych<sup>2</sup>, Leszek Łatka<sup>3</sup>, Hanna Myalska-Głowacka<sup>4</sup>

<sup>1</sup> Department of Engineering Materials and Biomaterials, Silesian University of Technology, ul. Konarskiego 18a, 44-100 Gliwice, Poland

<sup>2</sup> Institute of Manufacturing and Materials Technology, Faculty of Mechanical Engineering and Ship Technology, Gdańsk University of Technology, ul. Gabriela Narutowicza 11/12, 80-233 Gdańsk, Poland

<sup>3</sup> Department of Metal Forming, Welding and Metrology, Faculty of Mechanical Engineering, Wrocław University of Science and Technology, ul. Łukasiewicza 5, 50-371 Wrocław, Poland

<sup>4</sup> Department of Materials Engineering, Silesian University of Technology, ul. Krasińskiego 8, 40-019 Katowice, Poland

\* Corresponding author's e-mail: ewa.jonda@polsl.pl

## ABSTRACT

Cermet coatings are one of the best surface protection of machine elements against wear. On the other hand, the most universal and economically justified method of applying such coatings is high velocity oxy-fuel (HVOF) spraying. This method makes it possible to produce coatings characterized by compact structure, low porosity and very good adhesion to the substrate. All these fundamental properties contribute to the high wear resistance of these coatings. However, carrying out full wear tests (e.g. ball-on-disc) is time-consuming, especially when it is necessary to select the proper feedstock material and carefully selected process parameters. The aim of the following researches was to statistically investigate the possibility of replacing long-term wear resistance tests with estimation of this performance on the basis of determining the fundamental mechanical properties of the coatings. Three types of coating materials were selected: WC-12Co, WC-10Co-4Cr and WC-20Cr<sub>3</sub>C<sub>2</sub>-7Ni, which were deposited on AZ31 magnesium alloy substrates from three different spray distances: 320, 360 and 400 mm. On the basis of the tests carried out and using cluster analysis techniques (the Ward and k-means methods), the relative similarity between the obtained coatings was determined. The applied methodology allowed to select from the analyzed cermet coatings such samples that were characterized by improved resistance to abrasive wear. The obtained results of the analyzes were also referred to the results of tests of resistance to abrasive wear.

**Keywords:** cluster analysis, HVOF spraying, cermet coating, AZ31 magnesium alloy, mechanical properties, wear resistance.

## INTRODUCTION

The dynamic development of technology makes it necessary to look for new design solutions aimed at improving the level of efficiency and quality of the product, reducing dimensions and weight, as well as increasing its reliability and dimensional stability under operating conditions [1, 2]. Therefore, the main factor determining

competitiveness on the industrial market is the search for and introduction of innovative solutions and technologies [3, 4].

One of the most important features that determine the attractiveness of the product is its durability and reliability under operating conditions [5]. However, in specific applications and conditions in which it works, it is exposed to the negative impact of various factors, e.g. abrasive wear,

erosion and corrosion processes, resulting in a loss of its operational properties [6, 7]. Abrasive wear is the most common destruction process in industrial conditions, accounting for approximately 50% of cases, consisting in the separation of small particles of the surface layer caused by the presence of elements acting as abrasive in the friction nodes, which significantly reduces its properties [8]. Therefore, it is important to introduce solutions that allow achieving the expected high level of functional properties, which in most cases involves the need to use new or improve existing production or regeneration techniques. These techniques restore functional properties and at the same time can increase the durability of the surface even several times [9, 10]. The most intensively developed directions for increasing the operational and functional properties of machine and equipment components include the use of coatings by thermal spray technology, including high velocity oxy fuel spraying (HVOF) [11, 12]. The coating allows you to combine the beneficial properties of the core with the wear resistance, hardness and heat resistance of the coating, which is the case with light construction materials such as, among others, foundry magnesium alloys, which, despite many favorable properties (including low density and high strength), are characterized by low resistance to abrasive wear, which significantly limits the possibilities of their use in some applications [13, 14]. This technology enables the production of coatings from a very wide range of materials, including: cermet materials based on tungsten carbide (WC), where due to the low temperature achieved by the particles, the carbide transformation takes place to a small extent. Moreover, because tungsten carbide (WC) can be well wetted, among others, by cobalt (Co), nickel (Ni), iron (Fe) and cobalt-chromium (CoCr), cermet materials made on its basis are among the most commonly used [15]. The advantages of the HVOF spraying method include slight heating of the substrate material during coating application, which practically excludes microstructural changes and limits its deformation [16, 17]. Moreover, coatings produced by this method are characterized by high quality, good mechanical properties, low porosity (< 3%), good corrosion resistance and low stresses inside the coating. This thermal spraying method is mainly used to manufacture coatings with high resistance to abrasive wear, protection against high temperatures, erosion and corrosion [18, 19]. In the era of

Industry 4.0, each production process is controlled and its parameters are controlled and recorded, which leads to the collection of large amounts of data. Databases containing large data sets can be used to obtain valuable information using data mining techniques [20]. Cluster analysis methods are a group of statistical techniques included in Data Mining that allow for the comparison of multidimensional objects, i.e. characterized by many diagnostic features [21]. These methods are based on the basic idea of creating groups of objects that meet the assumption of maximizing the distance between groups and minimizing the distance between elements in the considered cluster [22]. This is implemented using various methods, including two basic ones: hierarchical and non-hierarchical method. In the first case, the formation of clusters involves agglomerative or divisive building clusters based on hierarchy, while in the second situation it is achieved using various algorithms organizing elements into clusters, e.g. by creating all the clusters simultaneously by partitioning the data [23]. Among the hierarchical methods, the leading role is played by various variants of the Ward method, and among the non-hierarchical ones, k-means algorithms are often used. The main purposes of using cluster analysis are: investigation of the underlying structure of a data (extracting information hidden in the data), classification (indicating the degree of similarity between data points) and compression (organizing and summarizing objects into understandable groups) [24]. Cluster analysis techniques have been used in many fields of science and technology, in solving many different technical, as well as humanistic, social and medical problems [25]. Coating manufacturing processes are described by many parameters [26, 27], so they can be treated as multidimensional objects. This justifies an attempt to use cluster analysis as a tool to describe the properties of coatings. On the other hand, in the literature there is a very low number of papers where cluster analysis is used for thermal spray coatings characterization. Only a few examples are mainly connected with Vickers indentation and failure behaviour [28, 29] and as additional tool for acoustic emission technique [30, 31]. The aim of the work was to verify the possibility of applying cluster analysis algorithms to predict the abrasive wear resistance of coatings sprayed using the HVOF method on a substrate made of AZ31 foundry magnesium alloy. Based on the results obtained from experimental tests

of abrasive wear, a preliminary assessment of the resistance of the produced coatings was made in order to predict their resistance to abrasive wear depending on the type of coating material used and the distance of the gun nozzle from the substrate material during the spraying process.

## MATERIALS AND METHODS

Three types of commercially available powders were tested as feedstock material: (i) WC-12wt.%Co (Amperit 558.074, Höganäs), (ii) WC-10wt.%Co-4wt.%Cr (Amperit 518.074, Höganäs) and (iii) WC-20wt.%Cr<sub>3</sub>C<sub>2</sub>-7wt.%Ni (Woka 3702-1, Oerlikon Metco). The powders were sintered and agglomerated, and the particle size range of each of them was from -45 to +15 μm. The detail information about powders characterization could be found in [32, 33]. The substrate material was AZ31 magnesium alloy. The samples dimensions were: 60 mm in diameter and 10 mm in the thickness. Before spraying the substrate surfaces were sand blasted and cleaned with ethanol. The deposition of coatings was carried out by high velocity oxy fuel (HVOF) process with a spray system JP 5000 TAFA (Indianapolis, USA) in the industry conditions (RESURS Company in Warsaw, Poland). The liquid fuel was kerosene with feed rate equal to 26.1 l/h, whereas oxygen flow rate was equal to 900 slpm. Powder feed rate was keep state at the level 70 g/min. The variable parameter was spray distance. The samples code was given in Table 1.

The obtained coatings were examined in terms of their topography as well as polished cross sections using scanning electron microscope, SEM (Supra 35, Zeiss, Oberkochen, Germany) and digital optical microscope, Keyence VHX6000 (Keyence International, Mechelen, Belgium). The SEM images were used to determine coatings porosity. Twenty images at 1000x magnifications at random locations were carried out. The porosity of deposited coatings was assessed using ImageJ

open source software (1.50i version) according to the ASTM E2109-01 standard. The microhardness of coatings was measured with Vickers penetrator under a load of 2.94 N (HV0.3) using the HV1000 hardness tester (Sinowon Innovation Metrology, Dongguan, China), according to the EN ISO 4516 standard. For each sample at least 10 imprints at the coatings cross section were made. Then, average values and standard deviations were calculated. On the other hand, instrumental indentation have been used because of finer structure for cermet coatings. The indentation testing was carried out on an NHT<sup>3</sup> nanoindenter (Anton Paar, Graz, Austria). All tests were carried out at room temperature, on the coating cross sections, according to the ISO 14577-4 standard. The maximum load value is 500 mN and the Oliver-Pharr method [34] was selected to calculate the coating hardness. Additionally, the instrumental Young's modulus was determined using the indentation technique. These values are calculated from the slope of the discharge portion of the load depth curve. In the current study, the maximum load values ranged from 50 to 500 mN in increments of 50 mN. Then, the value of Young's modulus is calculated according to the Chicot method [35] with some slight variations in [36]. Fracture toughness ( $K_{IC}$ ) was measured by Vickers indentation test according to ASTM C1421 standard. The detailed information could be found in [37]. The cohesion in the deposited coatings was estimated by scratch hardness ( $HS_L$ ) assessment. These measurements were carried out with MicroCombiTester (Anton Paar, Graz, Austria) which was equipped with Rockwell diamond indenter (tip radius equal to 0.2 mm). The detailed information about this methodology could be found in [38]. The tribological behaviours of the composite coatings and the reference metal alloy were investigated in dry sliding conditions at room temperature using a MFT-5000 apparatus (Rtec Instruments, San Jose, CA, USA). Measurements were

**Table 1.** The samples code and variable parameter values

Feedstock powder	Spray distance, mm		
	320	360	400
WC-12Co	SDA-I	SDA-II	SDA-III
WC-10Co-4Cr	SDB-I	SDB-II	SDB-III
WC-20Cr <sub>3</sub> C <sub>2</sub> -7Ni	SDC-I	SDC-II	SDC-III

performed by the ball-on-disc method according to the ASTM G99 standard. Before the tests, rectangular test specimens ( $25 \times 25$  mm), were ground and polished in order to achieve an average surface roughness (Ra) of around  $0.8 \mu\text{m}$ . The WC-Co counter ball diameter was set at 6 mm. The applied load, sliding speed, sliding distance, and radius were 50 N, 10 cm/s, 1000 m, and 3 mm, respectively. The detailed information could be found in [39]. The analyzes used a methodology known from the literature, consisting in the Ward's hierarchical grouping method, which allows, among others, determining the number of clusters and then the non-hierarchical k-means method [40]. The relative similarity between properties of the obtained coatings was determined in Statistica 13 software package based on input data. The analyzes were performed in the following order: data preparation (correlation verification, variability analysis, normalization, stimulation), analysis using the Ward method with Euclidean distance (creating a dendrogram and assessing the number of clusters stages supported by substantive analysis), analysis using the k-means method. Linear ordering based on the same data has also been done. The results of all analyzes were subjected to substantive analysis.

## RESULTS AND DISCUSSION

The SEM images of selected samples surface morphologies are presented in Figure 1. For all examples relatively smooth surface with single unmelted particles could be seen. In general it is a typical morphology for HVOF deposited cermet coating [41, 42]. Slightly differences connected with different spray distance are also similar like in [43]. The SEM images

of the samples cross-sections are presented in Figure 2. In all cases the coatings exhibit dense and homogenous structure with good adhesion to the substrate. It is characteristic for HVOF method of coatings deposition [44, 45]. The first group of the mechanical properties (porosity, microhardness and fracture toughness) of deposited coatings are collected in Table 2. Presented values indicate the influence of increasing spray distance on increasing porosity as well as fracture toughness and decreasing microhardness. This dependency and obtained values are relatively close to the literature data [46, 47]. On the other hand, the type of coatings material also influence on these properties. In this case cermets based on cobalt matrix exhibit higher hardness and fracture toughness values, whereas coatings with nickel matrix show lower porosity values. Explanation of these phenomena could be found in [48–50]. The second group of the mechanical properties (instrumental hardness, instrumental elastic modulus and cohesion in the coating) are collected in Table 3. In this case, the influence of the spray distance is clearly visible. With increasing distance the values of all parameters decreasing. Similar tendency could be found in [51, 52]. On the other hand, the material type is very interesting, because samples WC-Co-Cr exhibit the highest value of the elastic modulus and cohesion in the coating. It could be connected with strengthening cause by solid solution with chromium and cobalt [53, 54]. Also WC grains are very good wetted by these two metals, which improve cohesion in the coating [15, 55]. Table 4 shows a matrix with the values of correlation coefficients between all analyzed independent variables. All variables except  $P$  are highly correlated with the others. This is unfavorable from the point of view of

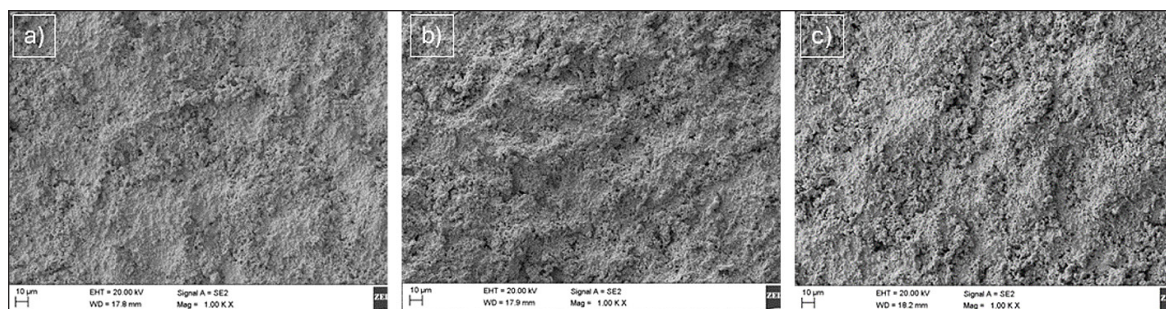


**Figure 1.** The SEM images of the surface topography for selected deposited coatings: a) SDA-I, b) SDA-II, c) SDA-III

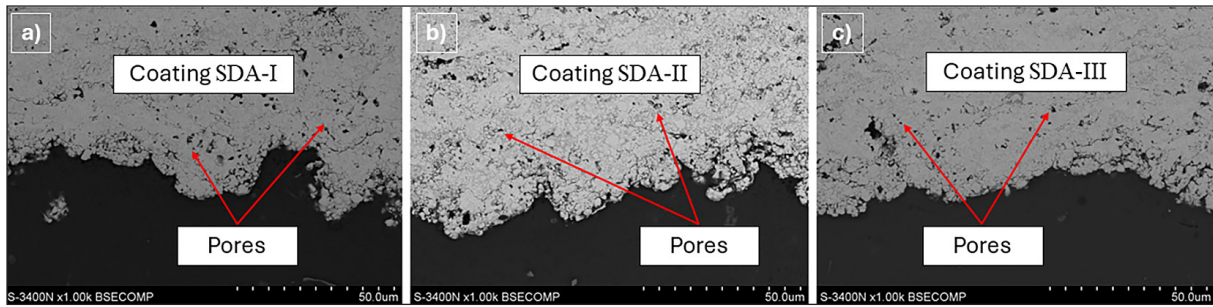


**Figure 2.** The SEM images of the cross-section for selected deposited coatings: a) SDA-I, b) SDA-II, c) SDA-III

**Table 2.** The average values of the porosity, microhardness and fracture toughness estimated for investigated coatings

Sample	Porosity, vol. %	Microhardness, HV0.3	Fracture toughness, $K_C$ , MPa·m <sup>1/2</sup>
SDA-I	1.9 ± 0.5	1305 ± 148	4.78 ± 0.47
SDA-II	2.6 ± 0.5	1296 ± 168	4.95 ± 0.54
SDA-III	2.8 ± 0.6	1085 ± 176	5.14 ± 0.49
SDB-I	2.3 ± 0.5	1278 ± 127	5.16 ± 0.46
SDB-II	2.9 ± 0.7	1198 ± 151	4.72 ± 0.68
SDB-III	3.1 ± 0.6	1042 ± 186	4.89 ± 0.62
SDC-I	1.3 ± 0.4	1027 ± 103	3.03 ± 0.29
SDC-II	1.9 ± 0.5	989 ± 108	3.14 ± 0.35
SDC-III	2.1 ± 0.5	990 ± 139	3.22 ± 0.36

**Table 3.** The average values of the instrumental hardness, instrumental elastic modulus and cohesion estimated for investigated coatings

Sample	Instrumental hardness $H_{IT}$ , GPa	Instrumental elastic modulus $E_{IT}$ , GPa	Cohesion parameter $H_{SL}$ , GPa
SDA-I	16.49 ± 2.04	339	4.5 ± 1.1
SDA-II	15.94 ± 2.15	333	4.7 ± 1.1
SDA-III	14.21 ± 2.37	330	4.0 ± 0.8
SDB-I	15.21 ± 1.97	346	5.5 ± 1.3
SDB-II	14.67 ± 1.82	341	5.3 ± 1.2
SDB-III	13.42 ± 2.25	334	4.8 ± 1.2
SDC-I	12.76 ± 1.77	312	4.1 ± 0.8
SDC-II	12.23 ± 1.29	305	3.8 ± 0.7
SDC-III	11.43 ± 1.88	301	3.5 ± 0.7

**Table 4.** Correlation matrix of diagnostic features

Diagnostic feature	$P$	$HV$	$K_C$	$H_{IT}$	$E_{IT}$	$H_{SL}$
P	1.00	0.19	0.73	0.26	0.54	0.45
HV	0.19	1.00	0.73	0.98	0.85	0.75
$K_C$	0.73	0.73	1.00	0.79	0.92	0.70
$H_{IT}$	0.26	0.98	0.79	1.00	0.86	0.67
$E_{IT}$	0.54	0.85	0.92	0.86	1.00	0.89
$H_{SL}$	0.45	0.75	0.70	0.67	0.89	1.00

**Note:**  $P$  – porosity, vol. %,  $HV$  – vickers hardness,  $K_C$  – fracture toughness, MPa·m<sup>1/2</sup>,  $H_{IT}$  – instrumental hardness, GPa,  $E_{IT}$  – instrumental elastic modulus, GPa,  $H_{SL}$  – cohesion parameter, GPa.

cluster analysis, but this is due to the nature of these studies, which describe the topography and mechanical properties of coatings in different ways. In the following analysis it is important to estimate discriminatory ability of the diagnostic features. For this reason the variability of features values was determined using the following relationship:

$$\omega = \frac{s_j}{x_j} \tag{1}$$

where:  $\omega$  – coefficient of variation,  $s_j$  – standard deviation,  $x_j$  – arithmetic mean of the feature value.

The results of above mentioned calculations are presented in Table 5. As it could be seen, all diagnostic features, except  $E_{IT}$ , are characterized by appropriate discriminatory ability (with  $\omega > 0.1$ ). A low value of feature variability could be the basis for excluding it from the analysis, but in this case it was decided to include it. Since it was assumed that all features are stimulants, they were normalized according to the relationship:

$$X'_{ij} = \frac{x_{ij} - \min(x_{ij})}{\max(x_{ij}) - \min(x_{ij})} \tag{2}$$

where:  $X'_{ij}$  – normalized value of the diagnostic feature,  $x_{ij}$  – value of the diagnostic feature.

Based on the test results listed in Table 6 as diagnostic features, three analyzes were performed for the following sets of diagnostic features based on the analysis of the thermal spraying process and coating properties: analysis I: Pn, HVn, KCn, HITn, EITn, and HSLn

(all), analysis II: Pn, KCn, HITn, EITn and HSLn, analysis III: Pn, HITn, and HSLn. Dendrograms illustrating the results of these analyzes are shown in Figure 3. In all three cases, two clusters can be distinguished: the first one covering three samples: SDC-I, SDC-II, SDC-III (cluster I) and the second grouping the remaining six samples: SDA-I, SDB-I, SDA-II, SDB-II, SDA-III, SDB-III (cluster II). The proposed division of the data set into clusters is marked in the plots with a dashed line. The distances between elements determining the degree of similarity in cluster II are different for each analysis. The results for cluster I are more homogeneous. The next stage of cluster analysis was to conduct the analysis using the non-hierarchical k-means method for the same sets of diagnostic features. The number of clusters (two) was assumed based on a previously conducted analysis using the Ward method. The initial cluster centers were determined according to the command: “choose observations to maximize initial between-cluster distances”. The results of the k-means analysis are shown in Figure 4. The results of linear ordering in the form of a plot are presented in Figure 5. Normalized index value was calculated based on the relationship:

$$w = \frac{\sum X'_{ij}}{n} \cdot 100\% \tag{3}$$

where:  $w$  – index value,  $X'_{ij}$  – normalized value of the diagnostic feature,  $n$  – number of diagnostic features.

**Table 5.** Coefficient of variation for diagnostic features

Diagnostic feature	$P$	$HV$	$K_C$	$H_{IT}$	$E_{IT}$	$H_{SL}$
Coefficient of variation, $\omega$	0.25	0.13	0.21	0.23	0.05	0.15

**Table 6.** Results of the diagnostic features in normalized form

Sample	$P$	$HV$	$K_C$	$H_{IT}$	$E_{IT}$	$H_{SL}$
SDA-I	0.33	1.00	0.82	1.00	0.84	0.50
SDA-II	0.72	0.98	0.90	0.89	0.71	0.60
SDA-III	0.83	0.47	0.99	0.55	0.64	0.25
SDB-I	0.56	0.94	1.00	0.75	1.00	1.00
SDB-II	0.89	0.74	0.79	0.64	0.89	0.90
SDB-III	1.00	0.37	0.87	0.39	0.73	0.65
SDC-I	0.00	0.33	0.00	0.26	0.24	0.30
SDC-II	0.33	0.24	0.05	0.16	0.09	0.15
SDC-III	0.44	0.00	0.09	0.00	0.00	0.00

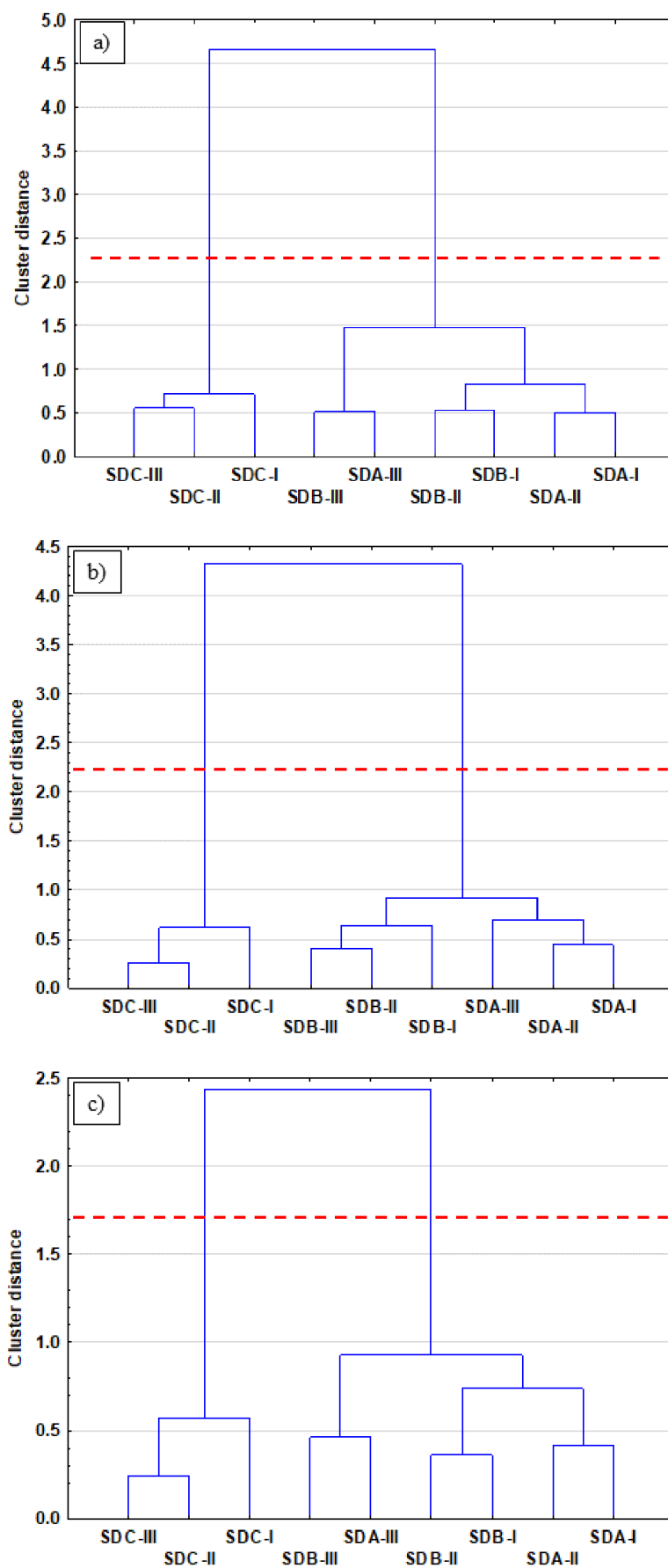


**Figure 3.** Euclidean distance dendrogram (Ward method) of coatings: (a) analysis I; (b) analysis II and (c) analysis III

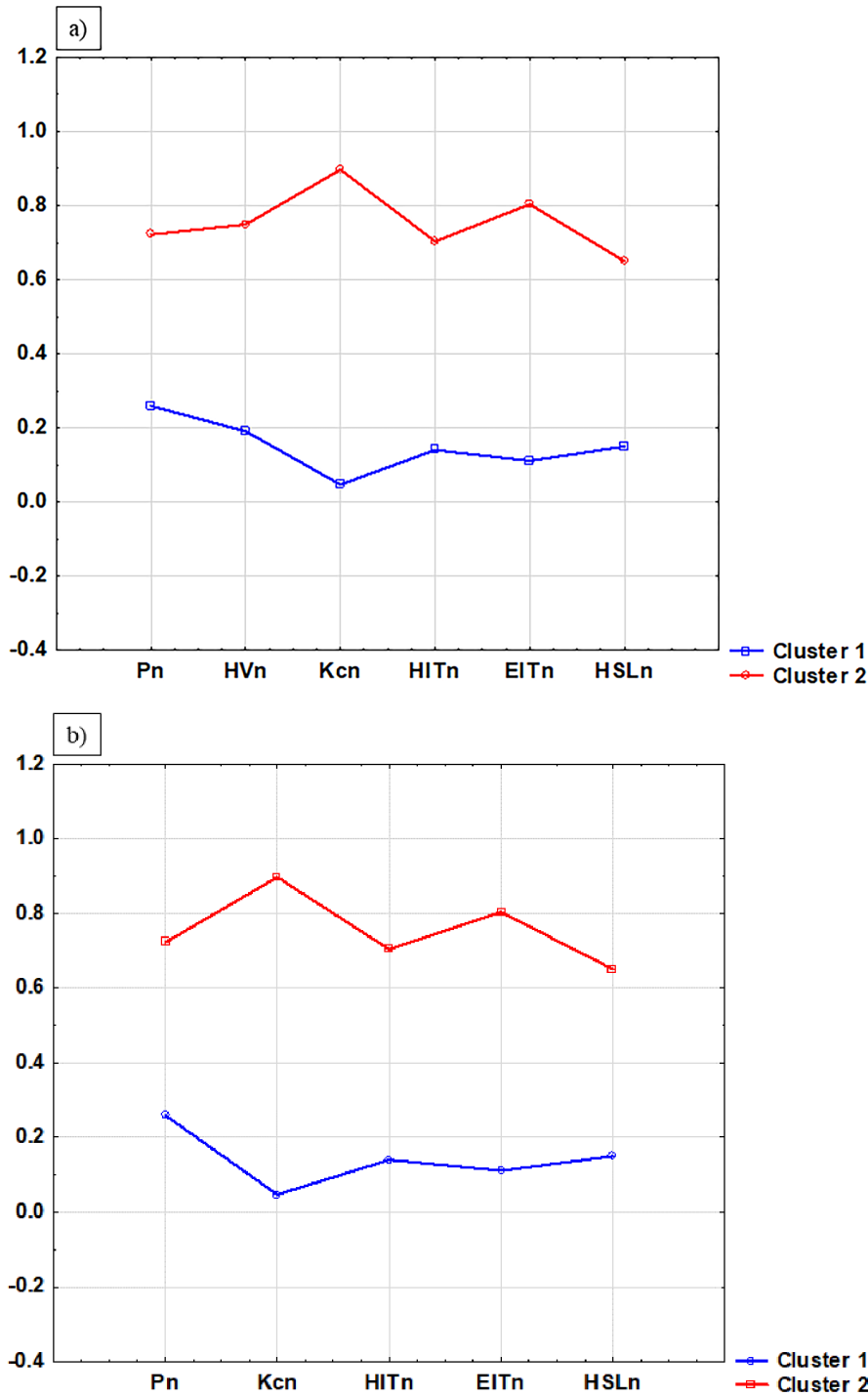


Figure 4. Plots of means for clusters: (a) analysis I; (b) analysis II and (c) analysis III

It is clearly visible that in this case also two clusters can be distinguished, including SDC-I, SDC-II and SDC-III elements (cluster I) and the remaining samples (cluster II). Based on this analysis, it can be assumed that the most resistant against wear is SDB-I sample and the least resistant is SDC-III one. The results obtained by carried out ball-on disc investigations, presented in the form of volumetric wear, strongly

confirmed the effects of the cluster analysis. The average values of wear factor ( $K$ ) for tested samples are presented in Table 7. As it could be seen the order is almost the same as in the Figure 5, which confirms the relatively high level of compatibility and correctness of the carried out analyzes. It is also a proof that cluster analysis could be used in order to describe the functional properties of thermally sprayed coatings.



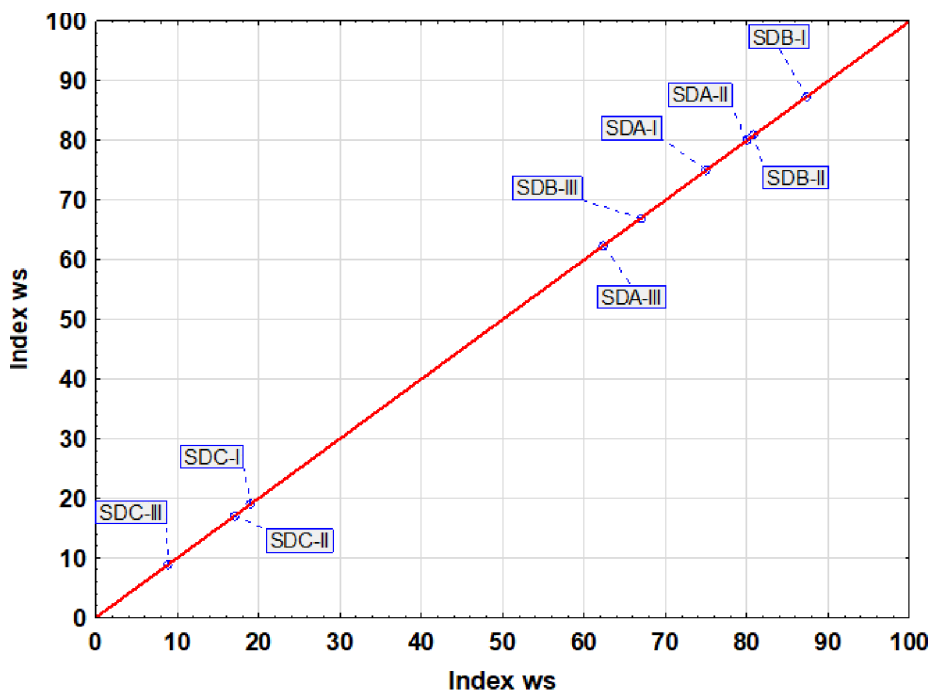


Figure 5. Linear ordering, scatterplot of normalized index for analysis II

Table 7. The average values of the wear factor, K ( $10^{-8} \text{ mm}^3/\text{N}\cdot\text{m}$ ) for tested coatings

Samples code								
SDA-I	SDA-II	SDA-III	SDB-I	SDB-II	SDB-III	SDC-I	SDC-II	SDC-III
9.1	7.7	9.6	5.6	6.2	8.4	12.3	14.4	17.8
(5)	(3)	(6)	(1)	(2)	(4)	(7)	(8)	(9)

Note: (1) – the best wear resistance; (9) – the worst wear resistance

## CONCLUSIONS

In this study, three commercial WC-based powders were deposited on the AZ31 magnesium alloy substrate by HVOF method. The variable process parameter was spray distance. The main research goal of the current paper was to check the statistical investigation possibilities of replacing long-term wear resistance tests with determination of this performance on the basis of determining the fundamental mechanical properties of the coatings. Selected mechanical properties were used as a diagnostic features in order to estimate wear resistance of the deposits. The successful of the developed methodology was proved. The following findings can be summarized:

- all cermet coatings exhibit dense and compact structure;
- the applied methodology allowed to select from the analyzed cermet coatings such samples that were characterized by improved resistance to abrasive wear;

- the obtained results of the analyzes were also referred to the results of tests of resistance to abrasive wear;
- the possibility of using cluster analysis methods for classification was positively verified.

It should be stressed that to the best Authors knowledge, carried out analysis is a very rare example of article devoted above mentioned issues.

## Acknowledgments

The research was financed by the rector’s pro-quality grant Silesian University of Technology, grant no. 10/010/RGJ24/1185.

## REFERENCES

1. Basile V., Tregua M., Giacalone M. A three-level view of readiness models: Statistical and managerial insights on industry 4.0. *Technology in Society* 2024; 77: 102528. <https://doi.org/10.1016/j.>

- techsoc.2024.102528
2. Ghasemi A., Farajzadeh F., Heavey C., Fowler J., Papadopoulos C.T. Simulation optimization applied to production scheduling in the era of industry 4.0: A review and future roadmap. *Journal of Industrial Information Integration* 2024; 39: 100599. <https://doi.org/10.1016/j.jii.2024.100599>
  3. Delke V., Schiele H., Buchholz W., Kelly S. Implementing Industry 4.0 technologies: Future roles in purchasing and supply management. *Technological Forecasting and Social Change* 2023; 196: 122847. <https://doi.org/10.1016/j.techfore.2023.122847>
  4. Javaid M., Haleem A., Singh R.P., Sinha A.K. Digital economy to improve the culture of industry 4.0: A study on features, implementation and challenges. *Green Technologies and Sustainability* 2024; 2: 100083. <https://doi.org/10.1016/j.grets.2024.100083>
  5. Kopeinig J., Woschank M., Olipp N. Industry 4.0 Technologies and their Implications for Environmental Sustainability in the Manufacturing Industry. *Procedia Computer Science* 2024; 232: 2777–89. <https://doi.org/10.1016/j.procs.2024.02.095>
  6. Menezes P.L., Nosonovsky M., Ingole S.P., Kailas S.V., Lovell M.R., editors. *Tribology for Scientists and Engineers: From Basics to Advanced Concepts*. New York, NY: Springer New York; 2013. <https://doi.org/10.1007/978-1-4614-1945-7>.
  7. Bhushan B. *Introduction to tribology*. Second edition. Chichester, West Sussex, United Kingdom: John Wiley & Sons Inc; 2013.
  8. Katiyar J.K, Rao T., Rani A.M.A., Sulaiman M.H., Davim J.P. *Tribology in Sustainable Manufacturing*. 1st ed. Boca Raton: CRC Press; 2023. <https://doi.org/10.1201/9781003363576>.
  9. Pawlowski L. *The science and engineering of thermal spray coatings*. Chichester, West Sussex: J. Wiley and sons; 2008.
  10. Dwivedi D.K. *Surface Engineering*. New Delhi: Springer India; 2018. <https://doi.org/10.1007/978-81-322-3779-2>.
  11. Fauchais P.L., Heberlein J.V.R., Boulos M.I. *Thermal Spray Fundamentals*. Boston, MA: Springer US; 2014. <https://doi.org/10.1007/978-0-387-68991-3>
  12. Tejero-Martin D., Rezvani Rad M., McDonald A., Hussain T. Beyond traditional coatings: a review on thermal-sprayed functional and smart coatings. *J Therm Spray Tech* 2019; 28: 598–644. <https://doi.org/10.1007/s11666-019-00857-1>
  13. Berger L.-M. Application of hardmetals as thermal spray coatings. *International Journal of Refractory Metals and Hard Materials* 2015; 49: 350–64. <https://doi.org/10.1016/j.ijrmhm.2014.09.029>
  14. Bhosale D.G., Rathod W.S., Rukhande S.W. Effect of counter faces on sliding wear behavior of WC-Cr<sub>3</sub>C<sub>2</sub>-Ni composite coating deposited by high velocity oxy fuel. *Materials Today: Proceedings* 2021; 41: 780–5. <https://doi.org/10.1016/j.matpr.2020.08.466>
  15. Gren M.A., Wahnström G. Wetting of surfaces and grain boundaries in cemented carbides and the effect from local chemistry. *Materialia* 2019; 8: 100470. <https://doi.org/10.1016/j.mtla.2019.100470>
  16. Ahmed R., Ali O., Berndt C.C., Fardan A. Sliding wear of conventional and suspension sprayed nanocomposite WC-Co coatings: An Invited Review. *J Therm Spray Tech* 2021; 30: 800–61. <https://doi.org/10.1007/s11666-021-01185-z>
  17. Singh J., Vasudev H., Szala M., Gill H.S. Neural computing for erosion assessment in Al-20TiO<sub>2</sub> HVOF thermal spray coating. *Int J Interact Des Manuf* 2023. <https://doi.org/10.1007/s12008-023-01372-y>
  18. Singh N., Mehta A., Vasudev H., Samra P.S. A review on the design and analysis for the application of Wear and corrosion resistance coatings. *Int J Interact Des Manuf* 2023. <https://doi.org/10.1007/s12008-023-01411-8>
  19. Ma H., Li D., Li J. Effect of spraying power on microstructure, corrosion and wear resistance of fe-based amorphous coatings. *J Therm Spray Tech* 2022; 31: 1683–94. <https://doi.org/10.1007/s11666-022-01403-2>
  20. Dogan A., Birant D. Machine learning and data mining in manufacturing. *Expert Systems with Applications* 2021; 166: 114060. <https://doi.org/10.1016/j.eswa.2020.114060>
  21. Capezza C., Centofanti F., Lepore A., Palumbo B. Functional clustering methods for resistance spot welding process data in the automotive industry. *Appl Stoch Models Bus & Ind* 2021; 37: 908–25. <https://doi.org/10.1002/asmb.2648>
  22. Kujawińska A., Rogalewicz M., Muchowski M., Stańkowska M. Application of Cluster Analysis in Making Decision About Purchase of Additional Materials for Welding Process. In: Torres Guerrero F, Lozoya-Santos J, Gonzalez Mendivil E, Neira-Tovar L, Ramirez Flores PG, Martin-Gutierrez J, editors. *Smart Technology*, 213, Cham: Springer International Publishing; 2018; 10–20. [https://doi.org/10.1007/978-3-319-73323-4\\_2](https://doi.org/10.1007/978-3-319-73323-4_2)
  23. Gashi M., Ofner P., Ennsbrunner H., Thalmann S. Dealing with missing usage data in defect prediction: A case study of a welding supplier. *Computers in Industry* 2021; 132: 103505. <https://doi.org/10.1016/j.compind.2021.103505>
  24. Govender P., Sivakumar V. Application of k-means and hierarchical clustering techniques for analysis of air pollution: A review (1980–2019). *Atmospheric Pollution Research* 2020; 11: 40–56. <https://doi.org/10.1016/j.apr.2019.09.009>
  25. Hu H., Liu J., Zhang X., Fang M. An Effective and

- Adaptable K-means Algorithm for Big Data Cluster Analysis. *Pattern Recognition* 2023; 139: 109404. <https://doi.org/10.1016/j.patcog.2023.109404>
26. Sirohi S., Kumar S., Pandey C. Characterization of damage in thermal barrier coating under different thermal cycle. *Materials Today: Proceedings* 2021; 38: 2110–6. <https://doi.org/10.1016/j.matpr.2020.04.539>
27. Górnik M., Jonda E., Nowakowska M., Łatka L. The effect of spray distance on porosity, surface roughness and microhardness of WC-10Co-4Cr coatings deposited by HVOF. *Advances in Materials Science* 2021; 21: 99–111. <https://doi.org/10.2478/adms-2021-0028>
28. Vignesh B., Oliver W.C., Kumar G.S., Phani P.S. Critical assessment of high speed nanoindentation mapping technique and data deconvolution on thermal barrier coatings. *Materials & Design* 2019; 181: 108084. <https://doi.org/10.1016/j.matdes.2019.108084>
29. Alroy R.J., Seekala H., Phani P.S., Sivakumar G. Role of high-speed nanoindentation mapping to assess the structure-performance correlation of HVOF-sprayed Cr<sub>3</sub>C<sub>2</sub>-25NiCr coating. *Surface and Coatings Technology* 2024; 481: 130652. <https://doi.org/10.1016/j.surfcoat.2024.130652>
30. Li C., Qiao X., Wang T., Weng W., Li Q. Damage evolution and failure mechanism of thermal barrier coatings under Vickers indentation by using acoustic emission technique. *Progress in Natural Science: Materials International* 2018; 28: 90–6. <https://doi.org/10.1016/j.pnsc.2017.12.002>
31. Qiao X., Weng W.X., Li Q. Acoustic emission monitoring and failure behavior discrimination of 8YSZ thermal barrier coatings under Vickers indentation testing. *Surface and Coatings Technology* 2019; 358: 913–22. <https://doi.org/10.1016/j.surfcoat.2018.12.024>
32. Jonda E., Łatka L., Godzierz M., Maciej A. Investigations of microstructure and corrosion resistance of WC-Co and WC-Cr<sub>3</sub>C<sub>2</sub>-Ni coatings deposited by HVOF on magnesium alloy substrates. *Surface and Coatings Technology* 2023; 459: 129355. <https://doi.org/10.1016/j.surfcoat.2023.129355>
33. Jonda E., Łatka L., Lont A., Gołombek K., Szala M. The effect of HVOF spray distance on solid particle erosion resistance of WC-based Cermets Bonded by Co, Co-Cr and Ni Deposited on Mg-alloy Substrate. *Adv Sci Technol Res J* 2024; 18: 115–28. <https://doi.org/10.12913/22998624/184025>
34. Oliver W.C., Pharr G.M. Measurement of hardness and elastic modulus by instrumented indentation: Advances in understanding and refinements to methodology. *J Mater Res* 2004; 19: 3–20. <https://doi.org/10.1557/jmr.2004.19.1.3>
35. Chicot D. Hardness length-scale factor to model nano- and micro-indentation size effects. *Materials Science and Engineering: A* 2009; 499: 454–61. <https://doi.org/10.1016/j.msea.2008.09.040>
36. Łatka L., Chicot D., Cattini A., Pawłowski L., Ambroziak A. Modeling of elastic modulus and hardness determination by indentation of porous yttria stabilized zirconia coatings. *Surface and Coatings Technology* 2013; 220: 131–9. <https://doi.org/10.1016/j.surfcoat.2012.07.025>
37. Jonda E., Łatka L., Godzierz M., Olszowska K., Tomiczek A. Microstructure, residual stress and mechanical properties of double carbides cermet coatings manufactured on AZ31 substrate by high velocity oxy-fuel spraying. *ArchivCivMechEng* 2024; 24: 61. <https://doi.org/10.1007/s43452-024-00867-z>
38. Łatka L., Cattini A., Chicot D., Pawłowski L., Kozerski S., Petit F., Denoirjean A. Mechanical properties of Yttria- and Ceria-stabilized zirconia coatings obtained by suspension plasma spraying. *J Therm Spray Tech* 2013; 22: 125–30. <https://doi.org/10.1007/s11666-012-9874-7>
39. Jonda E., Szala M., Sroka M., Łatka L., Walczak M. Investigations of cavitation erosion and wear resistance of cermet coatings manufactured by HVOF spraying. *Applied Surface Science* 2023; 608: 155071. <https://doi.org/10.1016/j.apsusc.2022.155071>
40. Garcia-Dias R., Vieira S., Lopez Pinaya W.H., Mechelli A. Clustering analysis. *Machine Learning, Elsevier* 2020; 227–47. <https://doi.org/10.1016/B978-0-12-815739-8.00013-4>
41. Agüero A., Camón F., García de Blas J., del Hoyo J.C., Muelas R., Santaballa A., Ulargui S., Vallés P. HVOF-Deposited WCCoCr as replacement for hard Cr in landing gear actuators. *J Therm Spray Tech* 2011; 20: 1292–309. <https://doi.org/10.1007/s11666-011-9686-1>
42. Komarov P., Jech D., Tkachenko S., Slámečka K., Dvořák K., Čelko L. Wetting behavior of wear-resistant WC-Co-Cr cermet coatings produced by HVOF: the role of chemical composition and surface roughness. *J Therm Spray Tech* 2021; 30: 285–303. <https://doi.org/10.1007/s11666-020-01130-6>
43. Tillmann W., Kuhnt S., Baumann I.T., Kalka A., Becker-Emden E.-C., Brinkhoff A. Statistical comparison of processing different powder feedstock in an HVOF thermal spray process. *J Therm Spray Tech* 2022; 31: 1476–89. <https://doi.org/10.1007/s11666-022-01392-2>
44. Hong S., Wu Y., Wu J., Zhang Y., Zheng Y., Li J., Lin J. Microstructure and cavitation erosion behavior of HVOF sprayed ceramic-metal composite coatings for application in hydro-turbines. *Renewable Energy* 2021; 164: 1089–99. <https://doi.org/10.1016/j.renene.2020.08.099>
45. Qiao L., Wu Y., Hong S., Long W., Cheng J. Wet

- abrasive wear behavior of WC-based cermet coatings prepared by HVOF spraying. *Ceramics International* 2021; 47: 1829–36. <https://doi.org/10.1016/j.ceramint.2020.09.009>
46. Sidhu H.S., Sidhu B.S., Prakash S. Mechanical and microstructural properties of HVOF sprayed WC–Co and Cr<sub>3</sub>C<sub>2</sub>–NiCr coatings on the boiler tube steels using LPG as the fuel gas. *Journal of Materials Processing Technology* 2006; 171: 77–82. <https://doi.org/10.1016/j.jmatprotec.2005.06.058>
47. Karaoglanli A.C., Oge M., Doleker K.M., Hotamis M. Comparison of tribological properties of HVOF sprayed coatings with different composition. *Surface and Coatings Technology* 2017; 318: 299–308. <https://doi.org/10.1016/j.surfcoat.2017.02.021>
48. Bolelli G., Berger L.-M., Bonetti M., Lusvarghi L. Comparative study of the dry sliding wear behaviour of HVOF-sprayed WC–(W,Cr)2C–Ni and WC–CoCr hardmetal coatings. *Wear* 2014; 309: 96–111. <https://doi.org/10.1016/j.wear.2013.11.001>
49. Matikainen V., Rubio Peregrina S., Ojala N., Koivuluoto H., Schubert J., Houdková Š., Vuoristo P. Erosion wear performance of WC-10Co4Cr and Cr<sub>3</sub>C<sub>2</sub>-25NiCr coatings sprayed with high-velocity thermal spray processes. *Surface and Coatings Technology* 2019; 370: 196–212. <https://doi.org/10.1016/j.surfcoat.2019.04.067>
50. Vashishtha N., Khatirkar R.K., Sapate S.G. Tribological behaviour of HVOF sprayed WC-12Co, WC-10Co-4Cr and Cr<sub>3</sub>C<sub>2</sub>-25NiCr coatings. *Tribology International* 2017; 105: 55–68. <https://doi.org/10.1016/j.triboint.2016.09.025>
51. Houdková Š., Bláhová O., Zahálka F., Kašparová M. The Instrumented Indentation Study of HVOF-Sprayed Hardmetal Coatings. *J Therm Spray Tech* 2012; 21: 77–85. <https://doi.org/10.1007/s11666-011-9677-2>
52. Chen Y., Wu Y., Hong S., Long W., Ji X. The effect of impingement angle on erosion wear characteristics of HVOF sprayed WC-Ni and WC-Cr<sub>3</sub>C<sub>2</sub>-Ni cermet composite coatings. *Mater Res Express* 2020; 7: 026503. <https://doi.org/10.1088/2053-1591/ab6d31>
53. Bolelli G., Berger L.-M., Börner T., Koivuluoto H., Lusvarghi L., Lyphout C., Markocsan N., Matikainen V., Nylén P., Sassatelli P., Trache R., Vuoristo P. Tribology of HVOF- and HVOF-sprayed WC–10Co-4Cr hardmetal coatings: A comparative assessment. *Surface and coatings technology* 2015; 265: 125–44. <https://doi.org/10.1016/j.surfcoat.2015.01.048>
54. Barletta M., Bolelli G., Bonferroni B., Lusvarghi L. Wear and corrosion behavior of HVOF-sprayed WC-CoCr coatings on al alloys. *J Therm Spray Tech* 2010; 19: 358–67. <https://doi.org/10.1007/s11666-009-9387-1>
55. Berger L.-M., Saaro S., Naumann T., Kašparova M., Zahálka F. Influence of feedstock powder characteristics and spray processes on microstructure and properties of WC–(W,Cr)2C–Ni hardmetal coatings. *Surface and Coatings Technology* 2010; 205: 1080–7. <https://doi.org/10.1016/j.surfcoat.2010.07.032>